Available online at www.sciencedirect.com
ScienceDirect
Bioorganic & Medicinal Chemistry Letters 17 (2007) 6354–6363
Bioorganic & Medicinal Chemistry Letters

Synthesis, antibacterial activity, and quantitative structure–activity relationships of new (*Z*)-2-(nitroimidazolylmethylene)-3(2*H*)-benzofuranone derivatives

Narges Hadj-esfandiari,[a] Latifeh Navidpour,[a] Hooman Shadnia,[b] Mohsen Amini,[a] Nasrin Samadi,[c] Mohammad Ali Faramarzi[d] and Abbas Shafiee[a,*]

[a]*Department of Medicinal Chemistry, Faculty of Pharmacy and Pharmaceutical Sciences Research Center, Tehran University of Medical Sciences, Tehran 14174, Iran*
[b]*Department of Chemistry, Carleton University, Ottawa, Ont., Canada K1S 5B6*
[c]*Department of Drug and Food Control, Faculty of Pharmacy and Pharmaceutical Sciences Research Center, Tehran University of Medical Sciences, Tehran 14174, Iran*
[d]*Department of Pharmaceutical Biotechnology, Faculty of Pharmacy, Tehran University of Medical Sciences, Tehran 14174, Iran*

Received 14 January 2007; revised 2 August 2007; accepted 18 September 2007
Available online 21 September 2007

Abstract—A new series of (*Z*)-2-(1-methyl-5-nitroimidazole-2-ylmethylene)-3(2*H*)-benzofuranones (**11a**–**p**) and (*Z*)-2-(1-methyl-4-nitroimidazole-5-ylmethylene)-3(2*H*)-benzofuranones (**12a**–**m**) were synthesized and assayed for their antibacterial activity against Gram-positive and Gram-negative bacteria. Most of the 5-nitroimidazole analogues (**11a**–**p**) showed a remarkable inhibition of a wide spectrum of Gram-positive bacteria (*Staphylococcus aureus*, *Streptococcus epidermidis*, *MRSA*, and *Bacillus subtilis*) and Gram-negative *Klebsiella pneumoniae*, whereas 4-nitroimidazole analogues (**12a**–**m**) were not effective against selected bacteria. The quantitative structure–activity relationship investigations were applied to find out the correlation between the experimentally evaluated activities with various parameters of the compounds studied. The QSAR models built in this work had reasonable predictive power and could be explained by the observed trends in activities.

The emergence of bacterial resistance to established antibiotics in community and hospital-acquired infections is an ever-growing concern. In particular, the big three Gram-positive species, *Staphylococcus*, *Enterococcus*, and *Streptococcus*, have all evolved resistant strains over the last few years: methicillin-resistant *Staphylococcus aureus* (MRSA) strains now account for over 40% of *S. aureus* infections in hospitals;[1] vancomycin-resistant entrococcal (VRE) infections have also increased substantially, with some strains resistant to all established antibiotics[2]; *Streptococcus pneumoniae* is the most common cause of community-acquired pneumoniae and is increasingly resistant to β-lactams and macrolids. For these reasons, there is an urgent need for new antibacterial agents.

The use of nitroheterocyclic drugs as antibacterial, antiprotozoal, and anti-cancer agents is well established. 5-Nitroimidazoles and 5-nitrofuranes are the classes of nitroheterocyclic drugs most used as antibacterials.[3] The distinguishing properties between these two subclasses are their reduction potentials. It has been proposed that the active damaging species, intermediates in the reduction process, is the one-electron nitro radical anion, which explains the relative cytotoxicity of these drugs under hypoxia.[4] This intermediate species interacts with DNA, causing strand breaks[5] with simultaneous release of thymine and thymidine phosphonates and helix destabilization. Although there is a large amount of experimental work on nitroimidazoles, they remain an area of active research interest.

Recently, a novel class of (*Z*)-2-(5-nitrofuran-2-yl-methylene)-3(2*H*)-benzofuranones **1** has been designed and exhibited very good in vitro antibacterial properties (Fig. 1).[6] In this regard, the QSAR analyses suggested that the benzofuranic moiety is an important structural

Keywords: Nitroimidazole; 3(2*H*)-Benzofuranone; Antibacterial; QSAR.
* Corresponding author. Tel.: +98 21 66406757; fax: +98 21 66461178; e-mail: ashafiee@ams.ac.ir

0960-894X/$ - see front matter © 2007 Elsevier Ltd. All rights reserved.
doi:10.1016/j.bmcl.2007.09.062

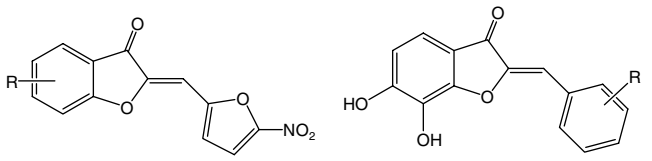

Figure 1. Representative examples of benzofuranone antimicrobials.

feature contributing to the activity. Furthermore, a series of (*Z*)-2-benzylidene-6,7-dihydroxy-3(2*H*)-benzofuranones **2** have shown antibacterial activity by inhibiting the chorismate synthase, a key enzyme in the shikimic acid pathway which is essential for the synthesis of aromatic amino acids in bacteria.[7] Considering the above results and as part of our ongoing program in developing new active antimicrobials against resistant bacteria,[8–13] we describe herein the synthesis and in vitro antimicrobial properties of a novel group of (*Z*)-2-(1-methyl-5-nitroimidazole-2-ylmethylene)-3(2*H*)-benzofuranones (**11a**–**p**) and (*Z*)-2-(1-methyl-4-nitroimidazole-5-ylmethylene)-3(2*H*)-benzofuranones (**12a**–**m**). To gain an insight into physicochemical and the structural features of this class of compounds that are important to the antibacterial activity, QSAR analyses of title compounds (**11** and **12**) were also performed.

Chemistry. The synthetic reactions used for the synthesis of substituted (*Z*)-2-(1-methyl-5-nitroimidazole-2-ylmethylene)-3(2*H*)-benzofuranones (**11a**–**p**), substituted (*Z*)-2-(1-methyl-4-nitroimidazole-5-ylmethylene)-3(2*H*)-benzofuranones (**12a**–**m**), (*E*)-2-(1-methyl-5-nitroimidazole-2-ylmethylene)-1-indanone (**15**), and indandione derivative (**16**) are outlined in Schemes 1–4.

3(2*H*)-Benzofuranones **8** are key intermediates for the production of the desired compounds (**11** and **12**). From our experience, the route shown in Scheme 1 summarizes the most convenient synthetic path leading to the 3(2*H*)-benzofuranones **8**. The latter was prepared starting from appropriate salicylic acid derivative **3**. Esterification of **3** with ethanol in the presence of sulfuric acid gave the ethyl salicylate **4**. Treatment of ethyl ester **4** with ethyl bromoacetate generated **5**,[14] which were hydrolyzed in basic media to produce **6**.[15] Ring closure of **6** in refluxing $AcOH/Ac_2O$ in the presence of sodium acetate followed by hydrolyzing acetyl ester in acidic media [HCl/H_2O/MeOH (1:10:40)] afforded the required 3(2*H*)-benzofuranones **8**.[16]

Title compounds, namely substituted (*Z*)-2-(1-methyl-5-nitroimidazole-2-ylmethylene)-3(2*H*)-benzofuranones (**11a**–**l** and **11n**) as well as indanone and indandione derivatives (**15**–**16**), were prepared by the condensation of appropriate 3(2*H*)-benzofuranone **8**, **1**-indanone **13** or 1,3-indandione **14**, respectively, with 1-methyl-5-nitro-2-carbaldehyde in acetic acid, in the presence of catalytic amount of sulfuric acid, while hydroxyl substituted (*Z*)-2-(1-methyl-5-nitroimidazole-2-ylmeth-

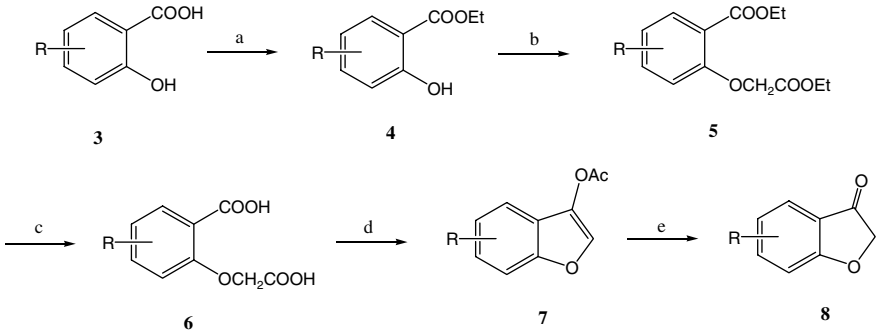

Scheme 1. Reagents and conditions: (a) EtOH (abs), H_2SO_4 (catalytic), reflux, 48 h; (b) $BrCH_2COOEt$, NaI, K_2CO_3, DMF, rt, 24 h; (c) KOH/MeOH (10%), reflux, 3 h; (d) sodium acetate, acetic acid/acetic anhydride, reflux, 4 h; (e) HCl/H_2O/MeOH (1:10:40), reflux, 1 h.

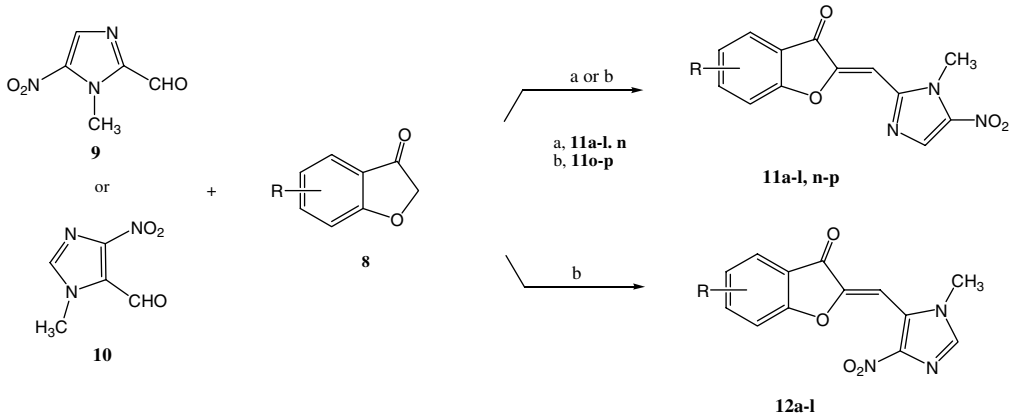

Scheme 2. Reagents and conditions: (a) acetic acid/sulfuric acid, 100 °C, 6 h; (b) acetic anhydride/anhydrous sodium acetate, 100 °C, 90 min.

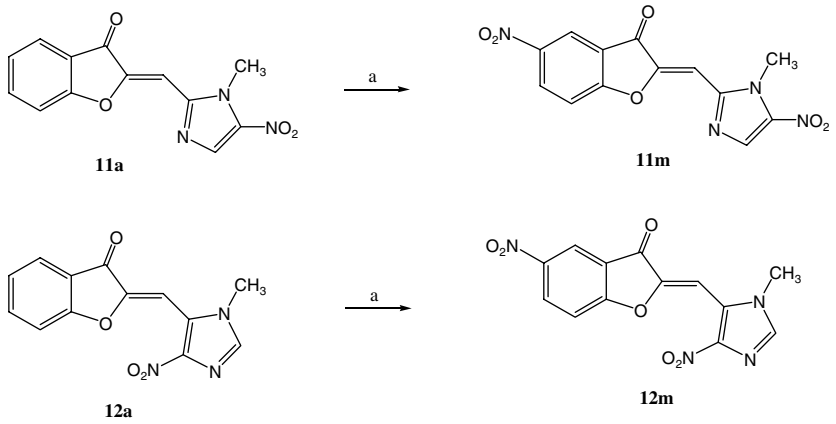

Scheme 3. Reagents and condition: (a) HNO_3, H_2SO_4, rt, 1 h.

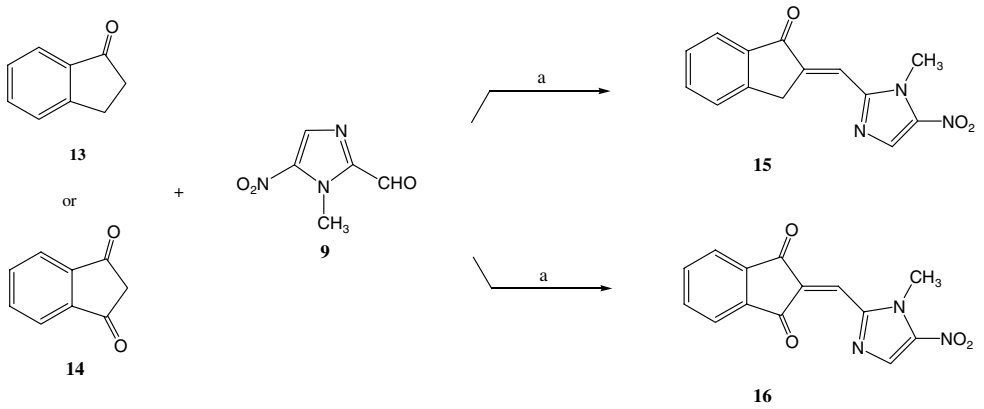

Scheme 4. Reagents and condition: (a) acetic acid/sulfuric acid, 100 °C, 6 h.

ylene)-3(2*H*)-benzofuranones (**11o**–**p**) and substituted (*Z*)-2-(1-methyl-4-nitroimidazole-5-ylmethylene)-3(2*H*)-benzofuranones (**12a**–**l**) were prepared by a different method in acetic anhydride in the presence of anhydrous sodium acetate (Scheme 2).[17,18] The nitro derivatives (**11m** and **12m**) were obtained by the treatment of the unsubstituted derivatives (**11a** and **12a**) with concentrated nitric acid in sulfuric acid (Scheme 3).[6]

Condensation gave single isomer as shown by NMR experiment. Precedent literature[19] suggested that *Z*-isomer would be obtained. The physicochemical data of the synthesized compounds (**11a**–**p**, **12a**–**m**, **15**, and **16**) are summarized in Table 1.

5-Nitrofuryl and phenyl derivatives of substituted 3(2*H*)-benzofuranones (**1**–**2**, Fig. 1) were prepared as reported previously.[6,7]

QSAR analysis. Even though these compounds do not build an ideal dataset for advanced QSAR studies (discussion follows), a simple QSAR study reveals satisfactory findings in terms of predictability of activities. Modeling and calculations were done on a 3.00 GHz Pentium 4 Machine.

Modeling: Structures of compounds **11a**–**p** and **12a**–**m** were sketched using builder module of MOE 2006.[20] A systematic conformational search was then performed (all rotatable bonds were rotated by 30 degree steps, RMS gradient = 0.01 (default), and RMS distance was reduced to 0.02). Generated conformers were optimized using MMFF94s[21,22] with born solvation model[23] and lowest energy conformer for each ligand was selected and used for QSAR analysis.

Dataset: To build the QSAR models, the logarithm of activities (1/MIC) was calculated. MIC = 100 μg/mL was used for the compounds which had a MIC > 100 μg/mL. The **QuaSAR** module of MOE was used to calculate molecular descriptors. These include the two-dimensional descriptors, and 3D descriptors as classified into i3D (internal coordinate dependent) and x3D (internal coordinate independent) descriptors.

The following descriptors were calculated: Kier topological descriptors defined by Kier and Hall (Kier1, Kier2, Kier3, KierA1, KierA2, KierA3, and Kierflex),[24] Molar refractivity (mr), molecular refractivity (including implicit hydrogens) using atomic contribution model (smr)[25] van der Walls surface area and its fractions (total: VSA, hydrogen bond acceptor: vsa_acc; hydrophobic: vsa_hyd, and polar: vsa_pol), principle moment of inertia (pmi), water accessible surface area and its fractions (ASA, ASA+, ASA−, ASA_H, ASA_P, CASA+, CASA−, FASA+, FASA−, FASA_H, FASA_P, FCA-

Table 1. Physicochemical data of **11a–p**, **12a–m**, **15**, and **16**

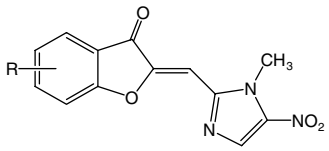

11a-p

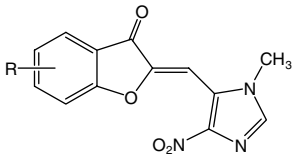

12a-m

Compound	R	Mp (°C)	Yield (%)	Molecular formula
11a	H	239–241	56	$C_{13}H_9N_3O_4$
11b	5-Cl	276–278	54	$C_{13}H_8ClN_3O_4$
11c	5-Br	254–257	62	$C_{13}H_8BrN_3O_4$
11d	5-Me	251–253	61	$C_{14}H_{11}N_3O_4$
11e	5-OMe	268–270	59	$C_{14}H_{11}N_3O_5$
11f	5-I	283–285	58	$C_{13}H_8IN_3O_4$
11g	6-Cl	266–268	46	$C_{13}H_8ClN_3O_4$
11h	6-Me	263–266	54	$C_{14}H_{11}N_3O_4$
11i	6-OMe	223–225	56	$C_{14}H_{11}N_3O_5$
11j	7-Cl	255–257	42	$C_{13}H_8ClN_3O_4$
11k	7-Me	229–231	55	$C_{14}H_{11}N_3O_4$
11l	7-OMe	235–237	48	$C_{14}H_{11}N_3O_5$
11m	5-NO_2	244–247	45	$C_{13}H_8N_4O_6$
11n	6,7-$(OMe)_2$	272–274	57	$C_{15}H_{13}N_3O_6$
11o	6-OH	242–244	52	$C_{13}H_9N_3O_5$
11p	4,6-$(OH)_2$	248–249	47	$C_{13}H_9N_3O_6$
12a	H	261–264	60	$C_{13}H_9N_3O_4$
12b	5-Cl	273–276	46	$C_{13}H_8ClN_3O_4$
12c	5-Br	267–269	45	$C_{13}H_8BrN_3O_4$
12d	5-Me	256–257	65	$C_{14}H_{11}N_3O_4$
12e	5-OMe	286–288	50	$C_{14}H_{11}N_3O_5$
12f	5-I	242–244	62	$C_{13}H_8IN_3O_4$
12g	6-Cl	283–285	26	$C_{13}H_8ClN_3O_4$
12h	6-Me	277–278	43	$C_{14}H_{11}N_3O_4$
12i	6-OMe	254–257	34	$C_{14}H_{11}N_3O_5$
12j	7-Cl	287–289	60	$C_{13}H_8ClN_3O_4$
12k	7-Me	266–268	52	$C_{14}H_{11}N_3O_4$
12l	7-OMe	265–267	41	$C_{14}H_{11}N_3O_5$
12m	5-NO_2	255–257	39	$C_{13}H_8N_4O_6$
15	—	270–272	56	$C_{14}H_{11}N_3O_3$
16	—	199–201	67	$C_{14}H_9N_3O_4$

SA+, and FCASA−), polar surface area calculated using group contributions (tpsa),[26] log of octanol/water partition coefficient (log *P*), globularity (glob), and van der Waals volume calculated using 0.75 Å grid (vol). For brevity, only the descriptors which were used in best models are shown in Table 2.

Data analysis method: An ideal dataset for a QSAR study should include numerous structures of diverse nature with proper span of activities. Our dataset included two classes of molecules, one of which was almost completely inactive. On average only 12 compounds were active on each organism. The activity span was not ideal either; about 65% inactive, 30% highly active, and only 5% moderately active (10 μg/mL < MIC < 99 μg/mL). Also, activity of all the inactive compounds was set to 100, an approximation that causes difficulty for fitting models. Despite these conditions, as it follows, a carefully designed basic QSAR reveals interesting findings, and practical predictability.

Running a non-biased fit on such a dataset leads to models that simply discriminate between the two classes of molecules (**11** vs **12**), especially when using several connectivity/geometrical descriptors. To avoid that, the data on active molecules were assigned a higher 'importance weight' (10) versus the inactive compounds (assigned weight = 1). Also, recruiting more than three descriptors was not allowed, which in turn limited the expected quality for best fits. Also using more than one geometrical/topological descriptor was not allowed.

Using the QuaSAR-Model in MOE, several PLS models were built in accordance with the remarked considerations. Performance criteria (RMSE: root mean square error and r^2: correlation coefficient for PLS models) were used to identify best models. The best models on each target organism are described in Table 3. Table 4 shows the predicted log activities using leave one out cross validation method (LOO), along with residual and *Z*-score values. Compounds having a *Z*-score of 2.5 or higher which are considered to be outliers to the fitted model and were excluded from regression models are shown. Figure 2a–e show the performance of these models as plot of experimental versus predicted log activities.

Lack of numerous 'moderately active' compounds makes it easy to build binary models in which the compounds are classified into active/inactive.[27] As expected, generally the same set of descriptors used to build PLS models was found to be proper for binary models. A binary threshold of 1.5 was used for logarithm of activities. Table 5 and Figure 3 show the details and performance of binary models. Performance of binary models is displayed as percentage of overall correct predictions (a) and its significance or *p*-value (s) which is interpreted as the likelihood of observing a result 'at least this extreme,' under the assumption that the model is doing no better than pure chance. The smaller the *p*-value, the less likely that the total accuracy is simply a chance. Also percentages of correctly predicted active/inactive molecules ($a1, a0$) and number of active versus inactive molecules (A/I) are given.

Results and discussion. The antibacterial properties of novel nitroimidazole derivatives were performed in vitro by a conventional agar-dilution method against a panel of selected Gram-positive and Gram-negative bacteria (Table 6).[28,29] The minimal inhibitory concentration (MIC, μg/mL) was determined in comparison with amoxicillin as the reference drug.

Generally, most 5-nitroimidazole analogues (**11a–m**) revealed respectable in vitro activity against Gram-positive and Gram-negative bacteria, while none of the compounds having 4-nitroimidazole moiety (**12a–m**) or phenyl group (**2**) exhibited any antibacterial activity up to the concentration of 100 μg/mL.

Having different cell wall structure, *Klebsiella pneumoniae*, a Gram-negative bacterium exhibited better susceptibility than Gram-positive bacteria, *Staphylococci*,

Table 2. Calculated descriptors which were used in derived models

Compound	Descriptor								
	Kier1	Kier2	Kier3	KierA2	KierA3	Dipole_*X*	vsa_pol	ASA_P	CASA−
2	13.959	5.780	2.741	3.907	1.820	0.199	43.205	126.620	617.920
11a	14.917	6.012	2.845	3.938	1.832	−0.559	21.753	142.901	672.267
11b	15.879	6.246	3.062	4.536	2.196	−0.147	21.753	143.269	816.828
11c	15.879	6.246	3.062	4.794	2.326	−0.240	21.753	143.066	863.307
11d	15.879	6.246	3.062	4.188	2.020	−0.660	21.753	143.608	604.296
11e	16.844	6.857	3.299	4.695	2.228	−0.562	24.257	182.955	657.101
11f	15.879	6.246	3.062	5.025	2.443	−0.232	21.753	141.771	869.485
11g	15.879	6.246	3.062	4.536	2.196	−0.325	21.753	143.265	821.169
11h	15.879	6.246	3.062	4.188	2.020	−0.640	21.753	143.610	611.035
11i	16.844	6.857	3.299	4.695	2.228	−0.406	24.257	179.016	652.113
11j	15.879	6.246	2.933	4.536	2.103	−0.775	21.753	144.341	807.527
11k	15.879	6.246	2.933	4.188	1.935	−0.597	21.753	142.567	597.650
11l	16.844	6.857	3.165	4.695	2.138	−0.970	24.257	180.622	650.245
11m	17.811	7.087	3.520	4.683	2.291	0.616	21.753	225.217	1057.487
11n	18.781	7.709	3.486	5.614	2.512	−0.245	26.761	211.055	617.069
11o	15.879	6.246	3.062	4.316	2.085	−0.554	35.320	203.545	762.599
11p	16.844	6.481	3.165	4.566	2.202	−0.065	48.887	238.637	847.682
12a	14.917	6.012	2.845	4.065	1.894	0.541	21.753	168.700	677.171
12b	15.879	6.246	3.062	4.670	2.264	0.264	21.753	169.555	839.293
12c	15.879	6.246	3.062	4.934	2.397	0.322	21.753	169.500	889.278
12d	15.879	6.246	3.062	4.316	2.085	0.579	21.753	169.278	621.771
12e	16.844	6.857	3.299	4.830	2.294	0.789	24.257	208.310	662.750
12g	15.879	6.246	3.062	4.670	2.264	0.479	21.753	169.530	828.592
12h	15.879	6.246	3.062	4.316	2.085	0.835	21.753	170.246	620.152
12i	16.844	6.857	3.299	4.830	2.294	0.808	24.257	209.360	671.420
12j	15.879	6.246	2.933	4.670	2.168	0.784	21.753	164.640	805.846
12k	15.879	6.246	2.933	4.316	1.997	0.819	21.753	162.861	598.414
12l	16.844	6.857	3.165	4.830	2.202	1.252	24.257	200.718	644.084
12m	17.811	7.087	3.520	4.813	2.357	0.039	21.753	249.183	1072.686
15	14.917	6.012	2.845	4.065	1.894	−0.528	19.249	149.941	680.556
16	15.879	6.246	2.813	4.092	1.811	−0.809	32.816	181.684	793.675

Table 3. Details of best PLS models ($n = 31$)

Organism	Model	r	r^2	RMSE	F[a]	q^2[b]	O[c]
S. aureus	$\log a = -4.95 + 4.43 * \text{Kier1} - 2.47 * \text{Dipole\_}X - 0.01 * \text{CASA}-$	0.84	0.76	0.88	87.77	0.62	2
S. epidermidis	$\log a = -4.95 + 4.43 * \text{Kier1} - 2.47 * \text{Dipole\_}X - 0.01 * \text{CASA}-$	0.85	0.79	0.89	69.53	0.72	2
MRSA	$\log a = -6.37 + 0.49 * \text{Kier3} - 0.51 * \text{Dipole\_}X - 0.49 * \text{CASA}-$	0.88	0.78	0.83	94.40	0.72	2
B. subtilis	$\log a = -5.52 + 4.7 * \text{Kier3} - 2.50 * \text{Dipole\_}X - 0.1 * \text{CASA}-$	0.85	0.72	1.09	98.59	0.77	2
K. pneumoniae	$\log a = -14.17 + 7.11 * \text{Kier 3} - 2.44 * \text{Dipole\_}X - 0.07 * \text{CASA}-$	0.88	0.77	1.13	62.94	0.70	2

[a] Fischer statistic.
[b] Cross validated square correlation coefficient.
[c] Number of outliers (determined using Z-scores of cross validation test, see Table 4).

and *Bacillus subtilis* to the action of 5-nitroimidazole analogues (**11a**–**p**). These compounds were inactive against *Pseudomonas aeruginosa* and *Escherichia coli*.[30] (*Z*)-2-(1-Methyl-5-nitroimidazole-2-ylmethylene)-3(2*H*)-benzofuranone (**11a**) was slightly superior in inhibiting the growth of *K. pneumoniae* (2- to 8-fold) than the Gram-positive bacteria.

Since the activity profiles of the compounds on target organisms are very similar (correlation coefficients $r^2 = 0.78$–0.99), it is understandable that the best QSAR models are very similar. Despite apparent robustness of these models, their accuracy for prediction of a new compound with a different structural backbone is unknown.

While Dipole_*X* is a good predictor, neither total dipole nor the other components of dipole vector (*Y* and *Z*) have comparable predictive power. Further analysis on compounds **11a**–**p** only (not shown here) suggests that this predictor does more than simple discrimination of compounds **11a**–**p** from compounds **12a**–**m**, so it is likely that the negative charge of $-NO_2$ group on C-5 of imidazole is necessary for action. Substitution of 5-nitroimidazole with 5-nitrofurane resulted in the compound with a slightly better inhibitory activity against *Staphylococci*

Table 4. Calculated log activities with residual and *Z*-score values for best PLS models

Structure	*S. aureus*			*S. epidermidis*			*MRSA*		
	clog(*a*)	Residual	*Z*-Score	clog(*a*)	Residual	*Z*-Score	clog(*a*)	Residual	*Z*-Score
2	1.215	−0.282	0.312	1.302	−0.369	0.403	1.097	−0.164	0.191
11a	2.683	1.780	2.187	2.876	1.588	1.871	2.754	1.016	1.225
11b	—	—	—	—	—	—	—	—	—
11c	1.399	−0.146	0.161	1.619	−0.366	0.400	1.361	−0.108	0.125
11d	4.803	−0.289	0.319	5.210	−0.697	0.768	4.836	−0.322	0.376
11e	5.197	−0.628	0.702	5.765	−1.197	1.358	5.283	−0.714	0.844
11f	1.278	0.101	0.111	1.497	−0.118	0.128	1.238	0.141	0.164
11g	2.075	−0.958	1.089	2.314	−1.197	1.362	2.051	−0.934	1.120
11h	4.673	−0.159	0.175	4.968	0.240	0.262	4.603	0.606	0.714
11i	4.648	0.616	0.687	5.195	0.068	0.074	4.730	0.534	0.626
11j	**2.203**	**2.380**	**3.208**	**2.419**	**2.164**	**2.742**	**2.156**	**2.428**	**3.584**
11k	4.015	0.499	0.555	4.195	1.014	1.136	4.014	0.500	0.586
11l	5.469	0.487	0.542	6.008	−0.052	0.056	5.533	0.424	0.496
11m	—	—	—	—	—	—	—	—	—
11n	5.586	−0.227	0.251	5.660	1.085	1.210	5.774	−0.416	0.485
11o	3.057	0.077	0.085	3.283	0.544	0.597	3.052	0.082	0.096
11p	1.640	−0.531	0.591	1.770	0.032	0.035	1.630	−0.521	0.611
11a	0.125	0.873	0.991	0.181	0.817	0.913	0.061	0.937	1.121
12b	0.323	0.795	0.902	0.470	0.647	0.723	0.284	0.833	0.996
12c	−0.311	1.564	1.786	−0.194	1.447	1.625	−0.361	1.614	1.944
12d	1.564	−0.516	0.585	1.795	−0.747	0.835	1.564	−0.515	0.615
12e	1.736	−0.633	0.718	2.094	−0.991	1.109	1.780	−0.678	0.809
12g	−0.137	1.254	1.428	−0.004	1.122	1.257	−0.178	1.295	1.555
12h	0.911	0.137	0.155	1.121	−0.073	0.081	0.905	0.143	0.171
12i	1.601	−0.499	0.565	1.952	−0.850	0.950	1.643	−0.540	0.645
12j	**−1.360**	**2.478**	**2.865**	**−1.335**	**2.453**	**2.790**	**−1.436**	**2.554**	**3.122**
12k	0.550	0.498	0.565	0.683	0.365	0.407	0.517	0.532	0.635
12l	0.009	1.094	1.243	0.245	0.858	0.959	0.014	1.089	1.304
12m	0.764	0.387	0.439	1.160	−0.009	0.010	0.794	0.357	0.426
15	**3.062**	**−2.072**	**2.663**	**3.245**	**−2.255**	**2.934**	**3.017**	**−2.026**	**2.775**
16	2.695	−1.654	1.978	2.623	−0.889	0.987	2.613	−1.572	1.980

Structure	*B. subtilis*			*K. pneumoniae*		
	clog(*a*)	Residual	*Z*-Score	clog(*a*)	Residual	*Z*-Score
2	0.430	0.504	0.452	−0.373	1.306	1.145
11a	—	—	—	5.363	1.182	1.045
11b	—	—	—	4.811	1.160	1.027
11c	2.501	−1.248	1.153	5.231	−0.512	0.444
11d	5.122	0.086	0.077	6.472	0.123	0.106
11e	6.271	−0.314	0.282	6.557	0.093	0.080
11f	**2.421**	**−1.042**	**0.953**	**5.414**	**−3.342**	**3.800**
11g	2.611	2.667	2.855	5.416	0.555	0.481
11h	4.925	0.977	0.891	6.405	0.190	0.164
11i	5.854	0.103	0.092	6.013	0.636	0.553
11j	2.777	1.806	1.724	6.647	−1.369	1.222
11k	3.934	1.275	1.179	5.831	0.764	0.666
11l	6.402	−0.446	0.400	7.821	−1.864	1.707
11m	0.811	2.419	2.302	3.867	0.057	0.049
11n	7.219	−0.475	0.426	5.257	2.156	2.003
11o	3.799	0.029	0.026	4.522	0.001	0.001
11p	2.948	−1.839	1.774	2.361	−1.252	1.095
12a	0.114	0.884	0.812	2.215	−1.217	1.078
12b	1.285	−0.168	0.154	3.693	−2.576	2.307
12c	0.791	0.462	0.424	3.514	−2.261	2.018
12d	2.034	−0.985	0.906	2.732	−1.684	1.496
12e	2.982	−1.879	1.738	2.349	1.526	1.355
12g	0.822	0.295	0.271	3.039	−1.921	1.710
12h	1.396	−0.348	0.319	1.932	−0.884	0.782
12i	2.870	−1.767	1.632	2.412	−1.309	1.160
12j	−0.778	1.895	1.752	1.700	−0.583	0.515
12k	0.609	0.439	0.403	1.593	−0.544	0.481
12l	0.905	0.197	0.181	0.559	0.544	0.481

(*continued on next page*)

Table 4 (*continued*)

Structure	*B. subtilis*			*K. pneumoniae*		
	clog(*a*)	Residual	*Z*-Score	clog(*a*)	Residual	*Z*-Score
12m	3.647	−2.496	2.322	—	—	—
15	3.020	−2.030	1.988	5.438	1.767	1.611
16	2.667	−0.933	0.847	—	—	—

Outliers (*Z*-scores above 2.5) are displayed in bold.

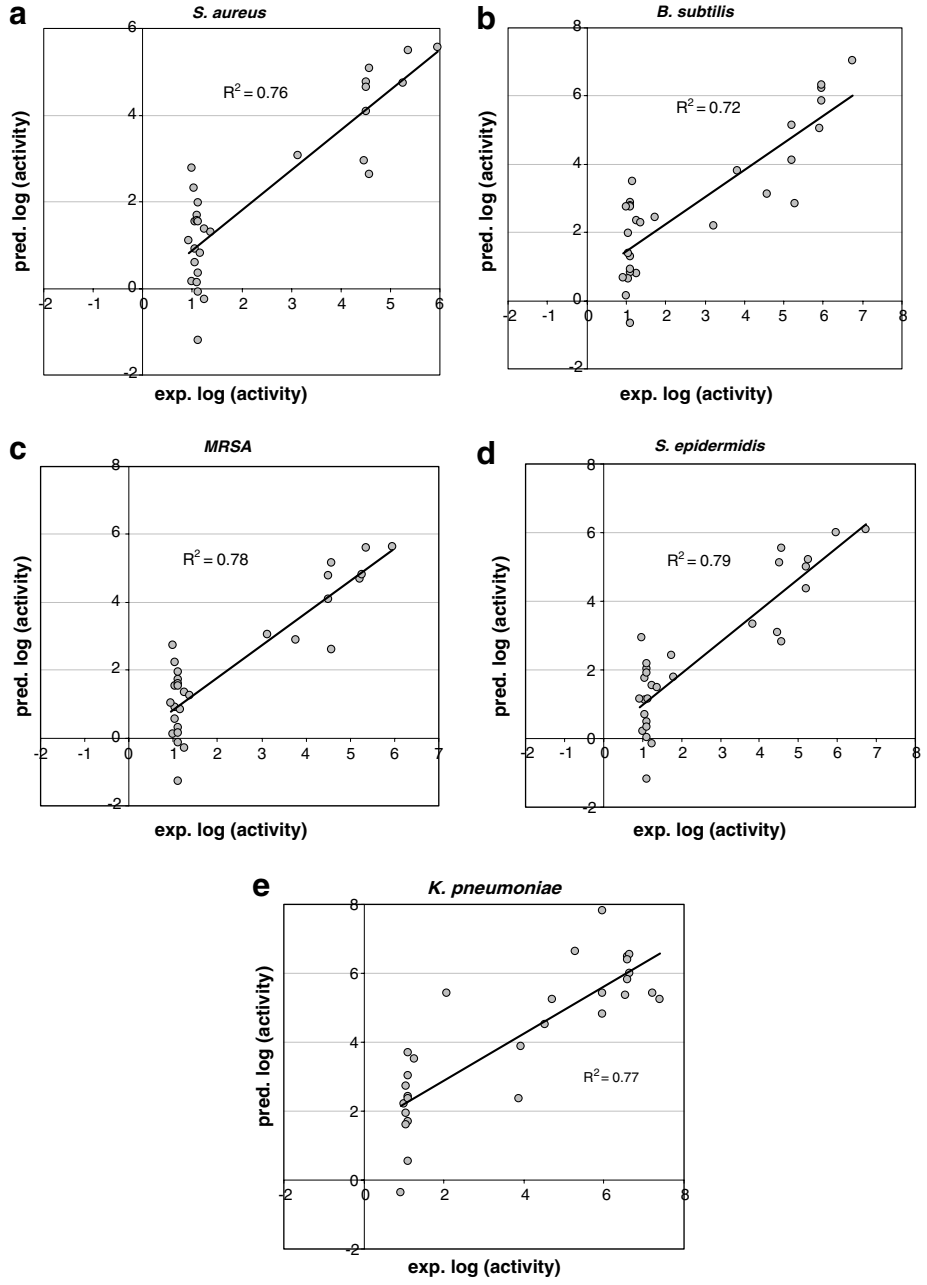

Figure 2. Performance of PLS models.

but less active (8-fold) against *B. subtilis* and inactive against Gram-negative ones.

vsa_pol or polar fraction of van der Waals surface area has a positive coefficient. Lack of correlation between vsa_pol and Dipole_*X* (overall $r^2 = 0.007$, for compounds **11a**–**p** which are generally active $r^2 = 0.17$) suggests a role for partial charges other than 5-nitro imidiazole. Partial charge on carbonyl oxygen in benzofuran is about −0.6 in comparison with −0.16 on the

Table 5. Details of best binary models

Organism	Descriptor	Importance	*A*/*I*	*a*	*a*1	*a*0	*S*
S. aureus	Dipole_*X*	0.50	12/19	94	83	100	3.4e−5
	KierA2	0.28					
	ASA_P	0.28					
S. epidermidis	Dipole_*X*	0.44	14/17	97	93	100	5.4e−6
	Kier1	0.45					
	ASA_P	0.27					
MRSA	Dipole_*X*	0.50	12/19	93	83	100	3.4e−5
	KierA3	0.13					
	vsa_pol	0.28					
B. subtilis	Dipole_*X*	0.56	14/17	97	93	100	5.4e−6
	KierA3	0.09					
	ASA_P	0.34					
K. pneumonia	Dipole_*X*	0.57	17/14	97	94	100	5.3e−6
	Kier2	0.44					
	ASA_P	0.61					

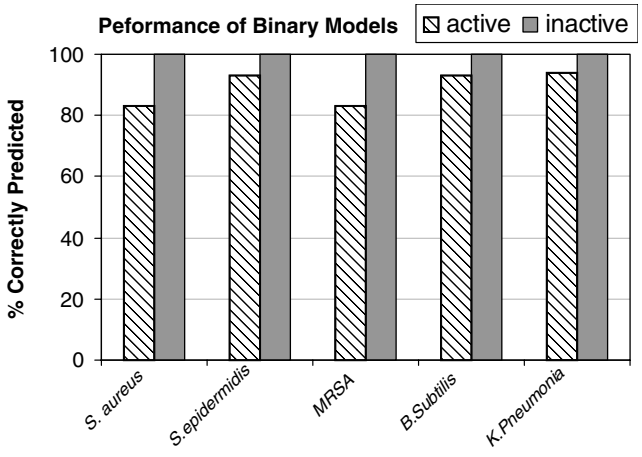

Figure 3. Performance of binary models.

ether oxygen which is partially eclipsed in *Z* conformers (especially in 7-substituted compounds as **11j**–**11l** which are generally active compounds), so it is likely that the second important partial charge is the carbonyl group of benzofuran system. Substitution of benzofuranone moiety with indanone and indandione (**15** and **16**) resulted in less to relatively inactive compounds. This phenomenon shows that the oxygen of benzofuranone ring could be the third important partial charge.

CASA− (Negative charge weighted surface area, times max negative charges)[31] has negative coefficient, penalizing extra negative charge on phenol ring (for example for nitro compounds **11m** and **12m**).

Adding one of the alpha-shaped descriptors (KierA2, KierA3) to previous two significantly increases the correlation coefficients (r^2 increase of 0.15–0.23) but when used alone (data not shown), these predictors have very low overall predictive power, suggesting their conditional (rather than additive) role. KierA2 and KierA3 are highest for 5-Br, 5-I and 5-nitro compounds (generally inactive compounds) and lowest for **11a**, **12a**. This might suggest that there is limited space available for this moiety of benzofuran system on target binding site. Thus, analogues having small substituents, such as chloro (**11b**), methyl (**11e**), and methoxy (**11f**), all exhibited similar inhibitory activity relative to unsubstituted benzofuran (**11a**), whereas the bulkier substituted analogues bearing bromo (**11c**) and iodo (**11d**) substituents proved to be inactive.

Among the different substituents on the C-5 position, compound **11m** having nitro substituent as an electron-withdrawing group revealed to be 2- to 8-fold less active than unsubstituted compound (**11a**).

For the more potent compounds, the effect of changing the position of substituent on the benzofuran moiety was then investigated. Generally, changing the position of substituents on the benzofuran appears to have little influence (2- to 4-fold) on antibacterial activity, with the exception for 6-chloro derivative (**11g**), shown to be inactive against *Staphylococci*. Among these analogues, compound **11n**, having two strong electron-donating group (OMe) at the 6 and 7 positions of the benzofuran moiety, was the most potent against Gram-positive and Gram-negative bacteria, with MIC values of 0.2–0.78 μg/mL. This compound was less potent against *S. aureus* and *S. epidermidis*, while exhibiting excellent inhibition against *MRSA*, and *B. subtilis* superior than reference drug, amoxicillin.

The most active compound, **11n**, has low CASA−, medium Dipole_*X* and high value of Kier descriptors, suggesting that large non-polar functional group on 7 position seems to be a good idea. KierA2, KierA3 are also high for halogenated compounds 5-Br, 5-I and 5-nitro compounds (generally inactive compounds) but these compounds have higher CASA− values.

Their spectrum of activity extended to penicillin-resistant *S. aureus* makes these compounds attractive antibacterial candidates also for treatment of infections caused by organisms resistant to currently available

Table 6. Antimicrobial activity by **1**–**2**, **11**–**12**, and **15**–**16**

Compound	R	MIC (μg/ml)				
		S. aureus[a]	*S. epidermidis*[b]	*MRSA*[c]	*B. subtilis*[d]	*K. pneumoniae*[e]
1	—	1.56	1.56	1.56	12.5	>100
2	—	>100	>100	>100	>100	>100
11a	H	3.125	3.125	6.25	0.78	0.39
11b	5-Cl	3.125	3.125	3.125	1.56	0.78
11c	5-Br	>100	>100	>100	>100	3.125
11d	5-I	>100	>100	>100	>100	50
11e	5-Me	3.125	3.125	3.125	1.56	0.39
11f	5-OMe	3.125	3.125	3.125	0.78	0.39
11g	6-Cl	>100	>100	>100	1.56	0.78
11h	6-Me	3.125	1.56	1.56	0.78	0.39
11i	6-OMe	1.56	1.56	1.56	0.78	0.39
11j	7-Cl	3.125	3.125	3.125	3.125	1.56
11k	7-Me	3.125	1.56	3.125	1.56	0.39
11l	7-OMe	0.78	0.78	0.78	0.78	0.78
11m	5-NO_2	12.5	6.25	12.5	12.5	6.25
11n	6,7-$(OMe)_2$	0.78	0.39	0.78	0.39	0.2
11o	6-OH[f]	12.5	6.25	12.5	6.25	3.12
11p	4,6-$(OH)_2$[f]	>100	50	>100	50	>100
12a	H	>100	>100	>100	>100	>100
12b	5-Cl	>100	>100	>100	>100	>100
12c	5-Br	>100	>100	>100	>100	>100
12d	5-I	>100	>100	>100	>100	>100
12e	5-Me	>100	>100	>100	>100	>100
12f	5-OMe	>100	>100	>100	>100	6.25
12g	6-Cl	>100	>100	>100	>100	>100
12h	6-Me	>100	>100	>100	>100	>100
12i	6-OMe	>100	>100	>100	>100	>100
12j	7-Cl	>100	>100	>100	>100	>100
12k	7-Me	>100	>100	>100	>100	>100
12l	7-OMe	>100	>100	>100	>100	>100
12m	5-NO_2	>100	>100	>100	>100	>100
15	—	>100	>100	>100	>100	0.2
16	—	100	50	100	50	>100
Amoxicillin	—	0.195	0.195	12.5	12.5	>100

[a] *Staphylococcus aureus* ATCC 6538p.
[b] *Staphylococcus epidermidis* ATCC 12228.
[c] Methicillin-resistant *Staphylococcus arueus* (clinically isolated).
[d] *Bacillus subtilis* ATCC 6633.
[e] *Klebsiella pneumoniae* ATCC 10031.
[f] The antimicrobial assay was performed in the presence of BHT 0.1%.

drugs. Moreover, most of the 5-nitro analogues showed excellent effectiveness against Gram-negative *K. pneumoniae*, better activity in respect to reference drug, amoxicillin.

In conclusion, a new series of substituted (*Z*)-2-arylidene-3(2*H*)-benzofuranones possessing 1-methyl-5-nitroimidazole (**11a**–**p**) or 4-nitroimidazole (**12a**–**m**) were synthesized and assayed for their antibacterial activity against Gram-positive and Gram-negative bacteria. Most of the 5-nitroimidazole analogues (**11a**–**p**) showed a remarkable inhibition of a wide spectrum of Gram-positive bacteria (*S. aureus*, *S. epidermidis*, *MRSA*, and *B. subtilis*) and Gram-negative *K. pneumoniae*, whereas 4-nitoimidazole analogues (**12a**–**m**) exhibited no effect against selected bacteria. The quantitative structure–activity relationship investigation was applied to find a correlation between different physicochemical parameters of the compounds studied and their biological activity. The predictive power of QSAR models built was confirmed by leave one out cross validation method. QSAR equations showed that Dipole_*X*, vsa_pol, KierA2, and KierA3 correlate significantly with the antibacterial activity, suggesting that possibly negative charge of –NO_2 group on C-5 of imidazole and partial charge on carbonyl oxygen in benzofuran are necessary for action. Moreover, there is a limited space available for this moiety of benzofuran system, thus the bulkier substituted analogues (**11c**–**d**) were inactive. Changing the position of the substituent on the benzofuran appears to have little influence on the antibacterial activity.

Acknowledgments

The authors sincerely thank Professor M. R. Ganjali for his kind collaborations. This work was supported by grants from the Research Council of Tehran University of Medical Sciences and INSF (Iran National Science Foundation).

References and notes

1. Public Health Laboratory Service. *Commun. Dis. Rep.* **2001**, *11*, 7.
2. Low, D. E.; Keller, N.; Barth, A.; Jones, R. N. *Clin. Infect. Dis.* **2001**, *32*, S133.
3. Edwards, D. I. DNA-Binding and Nicking Agents. In *Enzymes and other Molecular Targets*; Sammes, P. G., Taylor, J. B., Eds.; *Comprehensive Medicinal Chemistry. The Rational Design, Mechanistic Study & Therapeutic Application of Chemical Compounds*; Hansch, C., Ed.; Pergamon Press: Oxford, 1990; Vol. 2, pp 725–751.
4. Edwards, D. I. *J. Antimicrob. Chemother.* **1993**, *31*, 9.
5. Knight, R. C.; Skolimowski, I. M.; Edwards, D. I. *Biochem. Pharmacol.* **1978**, *27*, 2089.
6. Pires, J. R.; Saito, C.; Gomes, S. L.; Giesbrecht, A. M.; Amaral, A. T. *J. Med. Chem.* **2001**, *44*, 3673.
7. Thomas, M. G.; Lawson, C.; Allanson, N. M.; Leslie, B. W.; Bottomley, J. R.; McBride, A.; Olusanya, O. A. *Bioorg. Med. Chem. Lett.* **2003**, *13*, 423.
8. Foroumadi, A.; Ghodsi, S.; Emami, S.; Najjari, S.; Samadi, N.; Faramarzi, M. A.; Beikmohammadi, L.; Shirazi, F. H.; Shafiee, A. *Bioorg. Med. Chem. Lett.* **2006**, *16*, 3499.
9. Foroumadi, A.; Oboudiat, M.; Emami, S.; Karimollah, A.; Saghaee, L.; Moshafi, M. H.; Shafiee, A. *Bioorg. Med. Chem.* **2006**, *14*, 3421.
10. Foroumadi, A.; Emami, S.; Hassanzadeh, A.; Rajaee, M.; Sokhanvar, K.; Moshafi, M. H.; Shafiee, A. *Bioorg. Med. Chem. Lett.* **2006**, *15*, 4488.
11. Foroumadi, A.; Emami, S.; Mehni, M.; Moshafi, M. H.; Shafiee, A. *Bioorg. Med. Chem. Lett.* **2005**, *15*, 4536.
12. Foroumadi, A.; Pournourmohammadi, S.; Soltani, F.; Asgharian-Rezaee, M.; Dabiri, S.; Kharazmi, A.; Shafiee, A. *Bioorg. Med. Chem. Lett.* **2005**, *15*, 1983.
13. Tehranchian, S.; Akbarzadeh, T.; Fazeli, M. R.; Jamalifar, H.; Shafiee, A. *Bioorg. Med. Chem. Lett.* **2005**, *15*, 1023.
14. Edwards, C. R.; Readhead, M. J.; Tweddle, N. J. *J. Het. Chem.* **1987**, *24*, 495.
15. Robertson, A. *J. Chem. Soc.* **1932**, 1389.
16. Carvalho, C. F.; Sargebt, M. V. *J. Chem. Soc., Perkin Trans. 1* **1984**, 1605.
17. Rufer, C.; Kessler, H.-J.; Schröder, E.; Damerius, A. *Chim. Ther.* **1972**, *7*, 5.
18. Spectral data for compounds **11a** and **12a**. (*Z*)-2-(1-Methyl-5-nitroimidazole-2-ylmethylene)-3(2*H*)-benzofuranone (**11a**). Yield, 56%; mp 239–241 °C; IR (KBr): 1716 (CO), 1481, 1383 (NO_2) cm^{-1}; ^1H NMR (DMSO-d_6) δ 8.33 (s, 1H, H_4-imid), 7.98–7.20 (m, 4H, Ar), 6.87 (s, 1H, H-vinylic), 4.06 (s, 3H, NCH_3); MS m/z (%) 271 (M^+, 76), 225 (38), 184 (100), 155 (81), 127 (15), 101 (52), 76 (54), 50 (57). Anal. Calcd for $C_{13}H_9N_3O_4$: C, 57.57; H, 3.34; N, 15.49. Found: C, 57.40; H, 3.42; N, 15.63. (*Z*)-2-(1-Methyl-4-nitroimidazole-5-ylmethylene)-3(2*H*)-benzofuranone (**12a**). Yield, 60%; mp 261–264 °C; IR (KBr): 1716 (CO), 1501, 1347 (NO_2) cm^{-1}; ^1H NMR (DMSO-d_6) δ 8.04 (s, 1H, H_2-imid), 7.95–7.70 (m, 2H, Ar), 7.56–7.25 (m, 2H, Ar), 7.08 (s, 1H, H-vinylic), 3.82 (s, 3H, NCH_3); MS m/z (%) 271 (M^+, 4), 225 (26), 157 (9), 151 (89), 120 (100), 105 (20), 92 (72), 68 (97). Anal. Calcd for $C_{13}H_9N_3O_4$: C, 57.57; H, 3.34; N, 15.49. Found: C, 57.71; H, 3.47; N, 15.30.
19. Varma, R. S.; Varma, M. *Tetrahedron Lett.* **1992**, *33*, 5937.
20. MOE. Chemical Computing Group Inc., Montreal, Quebec, Canada, 2006, see http://www.chemcomp.com.
21. Halgren, T. A. *J. Comp. Chem.* **1999**, *20*, 720.
22. Halgren, T. A. *J. Comp. Chem.* **1999**, *20*, 730.
23. Bashford, D.; Case, D. *Annu. Rev. Phys. Chem.* **2000**, *51*, 129.
24. Hall, L. H.; Kier, L. B. *Rev. Comp. Chem.* **1991**, 2.
25. Ertl, P.; Rohde, B.; Selzer, P. *J. Med. Chem.* **2000**, *43*, 3714.
26. Wildman, S. A.; Crippen, G. M. *J. Chem. Inf. Comput. Sci.* **1999**, *5*, 868.
27. Labute, P. *Pac. Symp. Biocomput.* **1999**, *4*, 444.
28. Baron, E. J.; Finegolg, S. M.; In *Baily and Scott's Diagnostic Microbiology*, 8th ed.; Mosby, C. V., St. Louis, 1990; pp 184–188.
29. The antibacterial properties of **11o–p** which were oxidizable were performed in the presence of BHT 0.1% as an antioxidant. The antibacterial activity of BHT 0.1% was evaluated and no activity against any of the tested bacteria was observed.
30. The Gram-negative bacteria utilized in this study consisted of *Escherichia coli* ATCC 8739, *Pseudomonas aeruginosa* ATCC 9027, and *Klebsiella pneumoniae* ATCC 10031.
31. Stanton, D.; Jurs, P. *Anal. Chem.* **1990**, *62*, 2323.